PRAMANA
— journal of
physics

Vol. 85, No. 6
December 2015
pp. 1181–1191

Fission anisotropy of ^{197}Tl produced in fusion reactions in the framework of the modified statistical model

HADI ESLAMIZADEH

Department of Physics, Persian Gulf University, 75169 Bushehr, Iran
E-mail: m_eslamizadeh@yahoo.com

MS received 4 July 2014; revised 22 September 2014; accepted 27 September 2014
DOI: 10.1007/s12043-015-0956-1; ***e*Publication:** 6 November 2015

Abstract. The anisotropy of fission fragment angular distribution, evaporation residue cross-section and the fission cross-section were calculated for ^{197}Tl formed in ^{16}O+^{181}Ta reactions in the framework of the modified statistical model and the results were compared with the experimental data. The effects of temperature and projection of spin about the symmetry axis K have been considered for calculating potential energy surfaces and fission widths. It was shown that in the framework of the modified statistical model, by choosing appropriate values for the temperature coefficient of the effective potential, α, and scaling factor of the fission-barrier height, r_s, one can satisfactorily reproduce the above-mentioned experimental data. It was also shown that the appropriate values of these parameters for ^{197}Tl are $\alpha = 0.0185 \pm 0.0050$ MeV^{-2} and $r_s = 1.0006 \pm 0.0020$.

Keywords. Anisotropy of fission fragment; fission cross-section.

PACS Nos 25.70.Jj; 24.75.+i

1. Introduction

The fission of highly excited compound nuclei in heavy-ion-induced fusion reactions is an interesting subject in the current nuclear physics. For describing different features of nuclear fission, many researchers have used dynamical models based on Langevin or Fokker–Plank equations (see, e.g., [1–10]) or statistical models (e.g., [11–16]). The first statistical theory for nuclear fission was introduced by Bohr and Wheeler in 1931 [17]. Later, it has been found that the fission times calculated using this model over a wide range of excitation energies for a number of compound nuclei were less than the experimental data. Generally, it was accepted that several modifications are necessary for the Bohr and Wheeler's model. In terms of the Bohr and Wheeler model, the fission decay width was given by the following relation:

$$\Gamma_{\mathrm{f}}^{\mathrm{BW}} = \frac{1}{2\pi}\frac{1}{\rho_{\mathrm{CN}}(E^*)}\int_0^{E^*-B_{\mathrm{f}}} \rho_{\mathrm{sad}}(E^* - B_{\mathrm{f}} - \varepsilon)\mathrm{d}\varepsilon, \tag{1}$$

where ρ_{CN} and ρ_{sad} are the level densities of the compound nucleus at an excitation energy E^* at the ground and saddle points respectively and B_f is the height of the fission barrier. A number of modifications to the Bohr–Wheeler width have been proposed. The level density of the nuclear system is often estimated by assuming a weakly interacting Fermi gas and is approximately expressed as

$$\rho(E^* - \varepsilon) \approx \rho(E^*) \exp(-\varepsilon/T), \tag{2}$$

where $\rho(E^*)$ in terms of the level density parameter, $a(r)$, can be given as $\rho(E^*) \propto \exp(2\sqrt{a(r)E^*})$.

It can be shown that by substituting eq. (2) in eq. (1), the fission decay width can be given as

$$\Gamma_f^{BW} = \frac{T_{sad}\rho_{sad}(E^* - B_f)}{2\pi\rho_{CN}(E^*)}. \tag{3}$$

If the level density parameter is assumed to be a constant and if we use $E^* = aT^2$, then in the limit of a very high excitation energy or small barrier height the fission decay width can be given as

$$\Gamma_f^{BW} = (T_{sad}/2\pi) \exp(-B_f/T). \tag{4}$$

It should be noted that if the barrier height is large enough and the excitation energy is low then the temperatures at the ground state and the saddle point can be significantly different from each other. Therefore, for this case the fission width can be expressed as

$$\Gamma_f^{BW} = (T_{sad}/2\pi) \exp\left(\frac{-2B_f}{T_{gs} + T_{sad}}\right). \tag{5}$$

Furthermore, it can be shown that, if the Fermi gas level density parameter depends on the nuclear shape as

$$a(r) = a_v A + a_s A^{2/3} B_s(r), \tag{6}$$

then eq. (4) can be given by

$$\Gamma_f^{BW} = (\hbar\omega_{eq}/2\pi) \exp(-B_{eff}/T), \tag{7}$$

where ω_{eq} is the curvature of potential energy surface at the equilibrium position and B_{eff} is the height of the effective fission barrier. In eq. (6), A is the mass number of the compound nucleus, B_s is the dimensionless functional of the surface energy in the liquid-drop model, $a_v = 0.073\ \text{MeV}^{-1}$ and $a_s = 0.095\ \text{MeV}^{-1}$ [18].

The slowing effects of nuclear viscosity can be considered by the Kramers modification as [19]

$$\Gamma_f(K) = \left(\sqrt{1+\gamma^2} - \gamma\right) \times \frac{\hbar\omega_{eq}}{2\pi} \exp\left(-\frac{B_{eff}}{T}\right), \tag{8}$$

where K is the projection of spin J on the symmetry axis of the nucleus, γ is the dimensionless nuclear viscosity given by $\gamma = \beta/2\omega_{sp}$, β is the reduced nuclear dissipation coefficient, and ω_{eq}, ω_{sp} are the curvatures of the potential energy surface at the equilibrium position and the fission saddle point, respectively. B_{eff}, ω_{eq} and ω_{sp} are all assumed functions of K.

It is emphasized that eq. (8) is the fission width for a system with a fixed value of K. Therefore, the full fission decay width can be obtained by summing over all possible values of K [20]

$$\Gamma_{\rm f} = \frac{\sum_{K=-J}^{J} P(K)\Gamma_{\rm f}(K)}{\sum_{K=-J}^{J} P(K)}, \tag{9}$$

where $P(K) = (T/\hbar\omega_{\rm eq})\exp(-V_{\rm eq}/T)$ is the probability that the system is in a given K, $V_{\rm eq}$ is the potential energy at the equilibrium position as a function of K.

It should be stressed that in many statistical model codes [11–16], researchers used the ratio of the level density, a_f/a_n, and a scaling of the barrier heights, $f_{\rm B}$, which can be adjusted to reproduce experimental data. But fission process in heavy-ion reactions cannot be accurately modelled as a function of the excitation energy, using the Jdependence of the $T = 0$ fission barriers and a fixed value of a_f/a_n. In this study, we want to consider other parameters as free parameters which perform similar roles as a_f/a_n and $f_{\rm B}$ [20]. We consider the temperature coefficient in the effective potential formula, α, and a scaling of the modified liquid-drop model (MLDM) radii from their default values and use the values to calculate the surface and Coulomb energies with the parameter $r_{\rm s}$. The surface energy is proportional to the square of $r_{\rm s}$, while the Coulomb energy is inversely proportional to $r_{\rm s}$. Increasing $r_{\rm s}$ above one decreases the Coulomb energy but increases the surface energy. This causes the fission barriers to increase. The value $r_{\rm s}$ =1 is the standard MLDM value with fission-barrier heights in agreement with the finite-range liquid-drop model. The advantage of using $r_{\rm s}$ instead of $f_{\rm B}$ is that the curvature at the ground states and the fission transition points, the barrier locations and heights are all being determined in a self-consistent manner as a function of J, K and T. In this study, we use the modified statistical model similar to [20], to reproduce the experimental data on fission cross-section, evaporation residue cross-section and anisotropy of fission fragment angular distribution for ^{197}Tl formed in ^{16}O+^{181}Ta reactions.

This paper is organized as follows. In §2 we describe the model and basic equations. The results of the calculations are presented in §3. Finally, concluding remarks are given in §4.

2. Details of the model and basic equations

In this study, we use the statistical model as in [20] to simulate the fission process of ^{197}Tl produced in ^{16}O+^{181}Ta fusion reactions and reproduce the experimental data on the fission cross-section, evaporation residue cross-section and the anisotropy of fission fragment angular distribution for ^{197}Tl. In the present statistical model calculations, the effective potential is obtained based on the finite range liquid-drop model as in [20–23]:

$$\begin{aligned} V_{\rm eff}(r, A, Z, J, K) \;=\; & B_{\rm s}(r)E_{\rm s}^{0}(Z, A)(1 - \alpha T^2) + B_{\rm c}(r)E_{\rm c}^{0}(Z, A) \\ & + \frac{(J(J+1) - K^2)\hbar^2}{I_{\perp}(r)(4/5)MR_0^2 + 8Ma^2} \\ & + \frac{K^2\hbar^2}{I_{\|}(r)(4/5)MR_0^2 + 8Ma^2}, \end{aligned} \tag{10}$$

where E_s^0 and E_c^0 are the surface and Coulomb energies of the corresponding spherical system which can be determined as in [24,25]. $B_s(r)$ and $B_c(r)$ are surface and Coulomb energy terms and r is the distance between the centres of masses of the nascent fragments. $I_\perp$ and $I_\parallel$ are the moments of inertia with respect to the axes, perpendicular and parallel to the symmetry axis of the fissioning nucleus. M is the mass of the system, $R_0 = 1.2249A^{1/3}$ fm and $a = 0.6$ fm.

The magnitude of $\alpha = c_s A^{2/3}/E_s^0$ is very sensitive to the assumed properties of nuclear matter and other approximations [26]. Töke and Swiatecki [27] obtained $c_s \approx 0.27$ and other estimates of c_s gave values of α ranging from 0.007 to 0.022 MeV^{-2} [26,28–31].

It is shown that using an effective potential with a $(1 - \alpha T^2)$ dependence of the surface energy is a more complete approach and also for a given nucleus the height of fission barrier and location of the saddle point (transition point) depend on Z, A, J, K and T implying that the height of fission barrier and location of the fission transition point are functions of J, K and T.

Figures 1 and 2 show the potential energy surfaces calculated based on eq. (10) for the compound nucleus ^{197}Tl. Figure 1 shows the potential energy surface as a function of the collective coordinate r for different combinations of J and K values at $T = 2$ MeV and figure 2 shows the potential energy surface as a function of the collective coordinate r and K at $T = 2$ MeV and $J = 40\hbar$. It can be seen from figures 1 and 2 that the inclusion of the K coordinate changes not only the fission barrier height, but also affects the saddle point configuration. It is also clear from figure 1 that the height of the potential energy surface decreases with increasing spin of the nucleus and also, for a given value of spin, the height of the potential energy surface increases on increasing the value of K. Furthermore, it can be seen from figure 3 that the height of the potential energy surface decreases with the increase in temperature of the nucleus.

In the present calculations, we obtain the fission and decay widths for particle emission and the kind of nuclei decay during evolution is selected in terms of a standard Monte

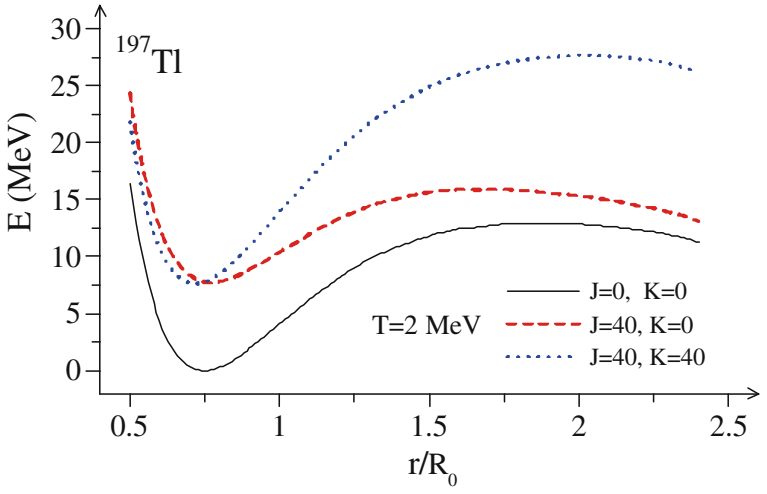

Figure 1. The potential energy surface for the compound nucleus ^{197}Tl as a function of the collective coordinate r, for different combinations of J and K values at $T = 2$ MeV. R_0 is the radius of the spherical nucleus.

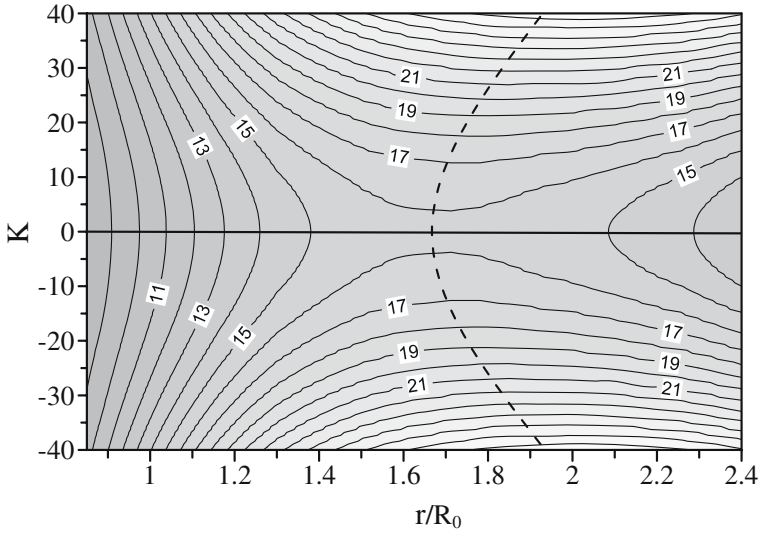

Figure 2. The potential energy surface for the compound nucleus ^{197}Tl as a function of the collective coordinate r and K at $T = 2$ MeV and $J = 40\hbar$. The numbers at the contour lines indicate the potential energy surface values (in MeV). The dashed line curve shows the dependence of saddle point deformations on K.

Carlo cascade procedure. After the evaporation of the pre-scission particle we recalculate the excitation energy and spin and continue the cascade procedure until the intrinsic energy becomes smaller than either the fission barrier height or the binding energy of a neutron. The angular momentum lost by the compound nucleus in the evaporation

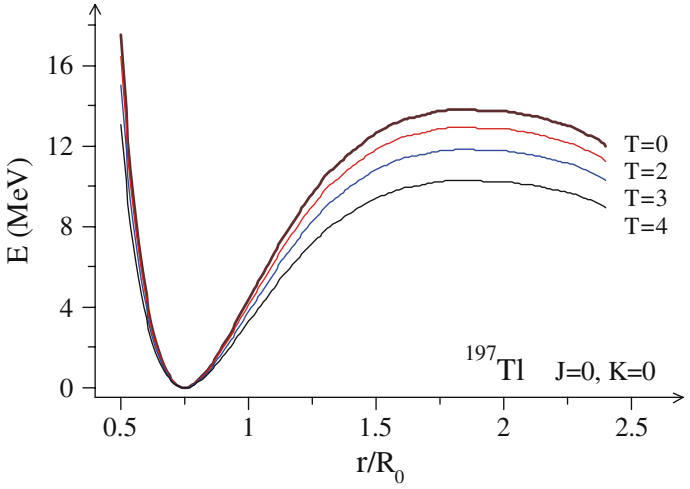

Figure 3. The potential energy surface for the compound nucleus ^{197}Tl as a function of the collective coordinate r at $T = 0, 2, 3, 4$ MeV, $J = 0\hbar$ and $K = 0\hbar$.

process is determined under the assumption that each neutron, proton or a γ quantum carries away $1\hbar$ while the α particle carries away $2\hbar$.

The particle emission width for a particle of kind ν can be calculated by [32]

$$\Gamma_\nu = (2s_\nu + 1)\frac{m_\nu}{\pi^2\hbar^2\rho_{\mathrm{C}}(E_{\mathrm{int}})}\int_0^{E_{\mathrm{int}}-B_\nu} \mathrm{d}\varepsilon_\nu \rho_{\mathrm{R}}(E_{\mathrm{int}} - B_\nu - \varepsilon_\nu)\varepsilon_\nu\sigma_{\mathrm{inv}}(\varepsilon_\nu). \quad (11)$$

Here s_ν is the spin of the emitted particle ν, m_ν is its reduced mass with respect to the residual nucleus, ρ_{C} and ρ_{R} are the level densities of the compound and residual nuclei, B_ν is the liquid-drop binding energies of the emitted particle ν, E_{int} is the intrinsic excitation energy of the parent nucleus and ε is the energy of the emitted particle. The inverse cross-sections, σ_{inv}, can be calculated as in [32]. We use the formula given by Lynn [33] for the calculation of the emission of giant dipole γ quanta

$$\Gamma_\gamma \cong \frac{3}{\rho_{\mathrm{C}}(E_{\mathrm{int}})}\int_0^{E_{\mathrm{int}}} \mathrm{d}\varepsilon\rho_{\mathrm{C}}(E_{\mathrm{int}} - \varepsilon)f(\varepsilon), \quad (12)$$

where $f(\varepsilon)$ can be calculated by

$$f(\varepsilon) = \frac{4}{3\pi}\frac{e^2}{\hbar c}\frac{1+M}{mc^2}\frac{NZ}{A}\frac{\Gamma_{\mathrm{G}}\varepsilon^4}{(\Gamma_{\mathrm{G}}\varepsilon)^2 + (\varepsilon^2 - E_{\mathrm{G}}^2)^2}, \quad (13)$$

with $E_{\mathrm{G}} = 80A^{-1/3}$ MeV and $\Gamma_{\mathrm{G}} = 5$ MeV being the position and width of the giant dipole resonance, M= 0.75 [34] and ε is the energy of the emitted γ-ray.

In our calculations for the determination of level density, we take into account the pairing corrections, collective vibrations and rotations in the nuclei as in [35,36].

In our simulation, the spin J is sampled from the spin distribution function as

$$\sigma(J) = \frac{2\pi}{k^2}\frac{2J+1}{1+\exp\ ((J - J_{\mathrm{c}})/\delta J)}, \quad (14)$$

where k, J_{c} and δJ are the wave number, critical spin for fusion and diffuseness, respectively. In the first approximation, J_{c} and δJ can be defined according to the scaled prescription [37]. The fission cross-section can be obtained in terms of the fusion cross-section as

$$\sigma_{\mathrm{Fiss}} = \sum_J \sigma_{\mathrm{Fus}}(J)\frac{\Gamma_{\mathrm{f}}}{\Gamma_{\mathrm{tot}}}. \quad (15)$$

In this paper, we use the standard transition state model to analyse the fission fragment angular distributions. This model assumes that there is a certain transition configuration for a fissile system that can be used to determine the angular distribution of the fission fragments. There are two assumptions on the position of the transition state and accordingly, we can consider two variants of the transition state model. These models are the saddle point transition model (SPTS) [38–40] and the scission point transition model (SCTS) [41–43]. In analysing the fission fragment angular distributions, it is usually assumed that fission fragments travel in the direction of the symmetry axis of the nucleus. Consequently, the fission fragment angular distributions can be determined by three quantum numbers: J, M, K where J is the spin of a compound nucleus, M is the projection of J on the axis of the projectile ion beam and K is the projection of J on the symmetry

axis of the nucleus. In the case of fusion of spinless ions, we have $M=0$. At fixed values of J and K, the angular distribution can be determined as

$$W(\theta, J, K) = (J + 1/2) \left| d^J_{M=0,K}(\theta) \right|^2, \tag{16}$$

where θ is the angle between the beam axis and the nuclear symmetry axis and the function $d^J_{M,K}(\theta)$ can be defined as in [38]. At large values of J, $W(\theta, J, K)$ can be approximated as

$$W(\theta, J, K) \approx \frac{J + 1/2}{\pi} \left[(J + 1/2)^2 \sin^2 \theta - K^2 \right]^{1/2}. \tag{17}$$

The angular distribution of fission fragments can be obtained by averaging eq. (16) over the quantum numbers J and K as

$$W(\theta) = \sum_{J=0}^{\infty} \sigma_J \sum_{K=-J}^{J} P(K) W(\theta, J, K). \tag{18}$$

Equation (18) shows that for calculating angular distribution, it is necessary to specify the type of distributions σ_J and $P(K)$ of the compound nuclei over J and K, respectively. In the SPTS and SCTS models an equilibrium distribution of K is assumed, and this is determined by the Boltzmann factor $\exp(-E_{\rm rot}/T)$ [43] at either the saddle point or the scission point, respectively. Therefore, the equilibrium distribution with respect to K has the form

$$P_{\rm eq}(K) = \frac{\exp(-K^2/(2K_0^2))}{\sum_{K=-J}^{J} \exp(-K^2/(2K_0^2))}, \tag{19}$$

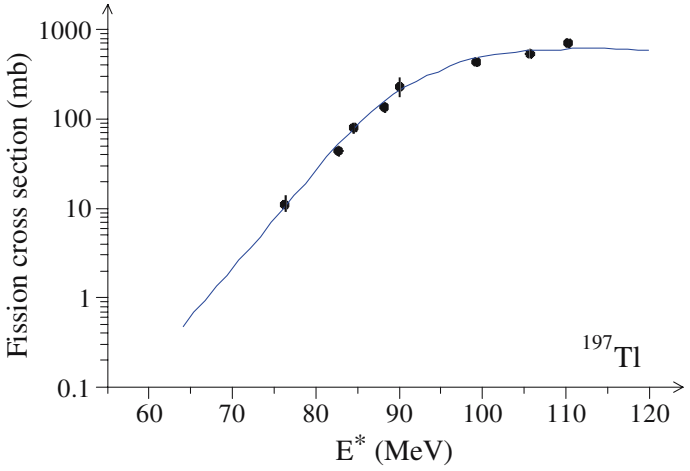

Figure 4. The results of fission cross-section (———) as a function of excitation energy for ^{197}Tl calculated by considering $\alpha = 0.0185 \pm 0.0050$ MeV^{-2} and $r_{\rm s} = 1.0006 \pm 0.0020$. The experimental data for fission cross-section (•) are taken from [45,46].

where the variance of equilibrium K distribution K_0 is determined by the expression

$$K_0^2 = \frac{T}{\hbar^2} I_{\text{eff}}, \qquad I_{\text{eff}} = \frac{I_\parallel I_\perp}{I_\perp - I_\parallel}, \tag{20}$$

where $I_\parallel$, $I_\perp$ are the parallel and perpendicular moments of inertia which are calculated at the transition state and T is the nuclear temperature.

The anisotropy of fission fragment angular distribution is given by

$$A = \frac{\langle W(180^\circ)\rangle}{\langle W(90^\circ)\rangle}. \tag{21}$$

It can be shown that the anisotropy of fission fragment angular distribution can be given by the approximate relation

$$\frac{\langle W(180^\circ)\rangle}{\langle W(90^\circ)\rangle} \approx 1 + \frac{\langle J^2\rangle}{4K_0^2}. \tag{22}$$

In our calculations, we use the magnitude of the reduced nuclear dissipation coefficient equal to 3×10^{21} s^{-1}. The required values of the parameter α are sensitive to changes in the assumed value of the reduced nuclear dissipation coefficient, but the required values of the parameter r_s are not very sensitive to changes.

In this study, as we are dealing with hot nuclei the shell corrections are supposed to be of minor importance. In other words, our results do not change substantially even if the shell corrections are considered. The fission fragment mass–energy distribution was

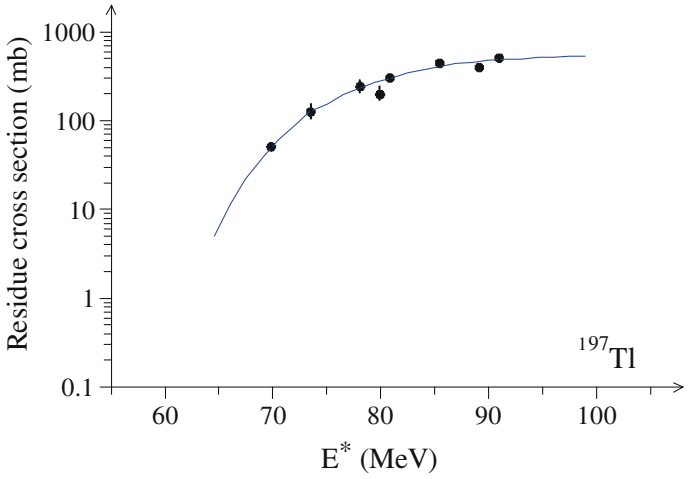

Figure 5. The results of evaporation residue cross-section (———) as a function of excitation energy for ^{197}Tl calculated by considering $\alpha = 0.0185 \pm 0.0050$ MeV^{-2} and $r_s = 1.0006 \pm 0.0020$. The experimental data for evaporation residue cross-section (•) are taken from [47].

analysed at low and medium excitation energies and it was demonstrated that the shell effects can be neglected above 50 MeV [44].

3. Results of the calculations and discussion

In this study, the fission cross-section, the evaporation residue cross-section and the anisotropy of fission fragment angular distribution have been calculated for ^{197}Tl formed in ^{16}O+^{181}Ta reactions. The anisotropy of fission fragment angular distribution for ^{197}Tl has been calculated in the framework of the SPTS model. In our calculations, the parameters α and r_s are adjusted to reproduce the single fission cross-section and the single evaporation residue cross-section at the same excitation energies for ^{197}Tl. Figures 4 and 5 show the results of fission cross-section and the evaporation residue cross-section as a function of excitation energy for ^{197}Tl. It can be seen from figures 4 and 5 that the results of the calculations are in good agreement with the experimental data when $\alpha = 0.0185 \pm 0.0050$ MeV^{-2} and $r_s = 1.0006 \pm 0.0020$.

Figure 6 shows the results of calculations of the anisotropy of fission fragment angular distribution for ^{197}Tl. It can be seen from figure 6 that by considering appropriate values for the parameters, α and r_s were obtained in the analysis of the fission cross-section and the evaporation residue cross-section can be satisfactorily reproduced from the experimental data on the anisotropy of fission fragment angular distribution for ^{197}Tl. Furthermore, the anisotropy of fission fragment angular distribution for ^{197}Tl was also calculated by considering $\alpha = 0$ and $r_s = 1$. It can be seen from figure 6 that the experimental data cannot be reproduced by considering $\alpha = 0$ and $r_s = 1$.

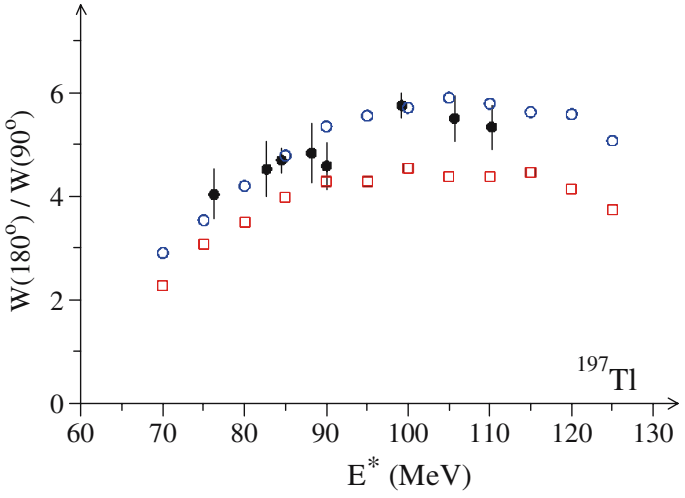

Figure 6. (○) The anisotropy of fission fragment angular distribution of ^{197}Tl calculated by considering $\alpha = 0.0185 \pm 0.0050$ MeV^{-2} and $r_s = 1.0006 \pm 0.0020$, (□) the results of anisotropy of fission fragment angular distribution calculated with $\alpha = 0$ and $r_s = 1$. The experimental data (●) are from [46,48].

4. Conclusions

The fission cross-section, evaporation residue cross-section and anisotropy of fission fragment angular distribution have been calculated for ^{197}Tl formed in ^{16}O+^{181}Ta reactions in the framework of the Kramers-modified statistical model, and results were compared with the experimental data. To calculate these quantities, the effects of temperature and projection of spin about the symmetry axis have been considered on the calculations of the potential energy surfaces and the fission widths.

In our calculations, the value of parameters α and r_s were adjusted to reproduce the single fission cross-section and the single evaporation residue cross-section at the same excitation energy for ^{197}Tl. It was shown that the results of fission and evaporation residue cross-sections are in good agreement with the experimental data when $\alpha = 0.0185 \pm 0.0050$ MeV^{-2} and $r_s = 1.0006 \pm 0.0020$. Then, we calculated the anisotropy of fission fragment angular distribution for ^{197}Tl. It was shown that the experimental data on the anisotropy of fission fragment angular distribution for ^{197}Tl can be satisfactorily reproduced by using $\alpha = 0.0185 \pm 0.0050$ MeV^{-2} and $r_s = 1.0006 \pm 0.0020$. Our result for α obtained for ^{197}Tl is consistent with the other studies [26,28–31]. Lestone and McCalla [20] provided a comprehensive discussion about their model, modified statistical model, and by analysing experimental data on the fission and evaporation residue cross-sections and the prescission neutron multiplicities, obtained information about α and r_s for ^{178}W, ^{188}Pt, ^{200}Pb, ^{210}Po and ^{213}Fr nuclie. In this study, we obtained appropriate values of α and r_s for ^{197}Tl. Furthermore, we studied the ability of the modified statistical model together with the saddle point transition model to analyse the experimental data on the anisotropy of fission fragment angular distribution for ^{197}Tl.

Acknowledgement

The support of the Research Committee of the Persian Gulf University is greatly acknowledged.

References

[1] P N Nadtochy, E G Ryabov, A E Gegechkori, Yu A Anischenko and G D Adeev, *Phys. Rev. C* **89**, 014616 (2014)
[2] H Eslamizadeh, *J. Phys. G: Nucl. Part. Phys.* **39**, 085110 (2012)
[3] H Eslamizadeh, *J. Phys. G: Nucl. Part. Phys.* **40**, 095102 (2013)
[4] P N Nadtochy, A Kelić and K-H Schmidt, *Phys. Rev. C* **75**, 064614 (2007)
[5] P N Nadtochy, E G Ryabov, A E Gegechkori, Yu A Anischenko and G D Adeev, *Phys. Rev. C* **85**, 064619 (2012)
[6] W Ye, *Int. J. Mod. Phys. E* **23**, 1460003 (2014)
[7] W Ye and N Wang, *Phys. Rev. C* **86**, 034605 (2013)
[8] H Eslamizadeh, *Pramana – J. Phys*. **78**, 231 (2012)
[9] H Eslamizadeh, M Pirpour, *Chin. Phys. C* (HEP& NP) **38**, 064101 (2014)
[10] H Eslamizadeh, *Pramana – J. Phys*. **80**, 621 (2013)
[11] F Pulnhofer, *Nucl. Phys. A* **280**, 267 (1977)
[12] M Blann and T A Komoto, Lawrence Livermore National Laboratory Report No. UCID 19390 (1982)

[13] M Blann and J Bisplinghoff, Lawrence Livermore National Laboratory Report No. UCID 19614 (1982)
[14] A Gavron, *Phys. Rev. C* **21**, 230 (1980)
[15] H Rossner, D Hilscher, D J Hinde, B Gebauer, M Lehmann, M Wilpert and E Mordhorst, *Phys. Rev. C* **40**, 2629 (1989)
[16] J P Lestone *et al*, *Nucl. Phys. A* **559**, 277 (1993)
[17] N Bohr and J A Wheeler, *Phys. Rev. C* **56**, 426 (1939)
[18] A V Ignatyuk, M G Itkis, V N Okolovich, G N Smirenkin and A S Tishin, *Yad. Fiz.* **21**, 1185 (1975)
[19] H A Kramers, *Physica* **7**, 284 (1940)
[20] J P Lestone and S G McCalla, *Phys. Rev. C* **79**, 044611 (2009)
[21] J P Lestone, *Phys. Rev. C* **59**, 1540 (1999)
[22] J P Lestone, *Phys. Rev. C* **51**, 580 (1995)
[23] A J Sierk, *Phys. Rev. C* **33**, 2039 (1986)
[24] W D Myers and W J Swiatecki, *Nucl. Phys.* **81**, 1 (1966)
[25] W D Myers and W J Swiatecki, *Ark. Fys.* **36**, 343 (1967)
[26] J P Lestone, *Phys. Rev. C* **52**, 1118 (1995)
[27] J Töke and W J Swiatecki, *Nucl. Phys. A* **372**, 141 (1981)
[28] A V Ignatyuk *et al*, *Yad. Fiz.* 1185 (1975); *Sov. J. Nucl. Phys*. **21**, 612 (1975)
[29] W Reisdorf, *Z. Phys. A* **300**, 227 (1981)
[30] M Prakash, J Wambach and Z Y Ma, *Phys. Lett. B* **128**, 141 (1983)
[31] S Shlomo, *Nucl. Phys. A* **539**, 17 (1992)
[32] M Blann, *Phys. Rev. C* **21**, 1770 (1980)
[33] J E Lynn, *The theory of neutron resonance reactions* (Clarendon, Oxford, 1968) p. 325
[34] V G Nedoresov and Yu N Ranyuk, *Fotodelenie yader za gigantskim rezonansom* (Kiev, Naukova Dumka, 1989) (in Russian)
[35] A V Ignatyuk, K K Istekov and G N Smirekin, *Sov. J. Nucl. Phys.* **29**, 875 (1979)
[36] A V Ignatyuk, *Statistical properties of excited atomic nuclei* (Energoatomizdat, Moscow, 1983)
[37] P Fröbrich and I I Gontchar, *Phys. Rep.* **292**, 131 (1998)
[38] H H Rossner *et al*, *Phys. Rev. Lett.* **53**, 38 (1984)
[39] P D Bond, *Phys. Rev. C* **32**, 471 (1985)
[40] H H Rossner *et al*, *Phys. Rev. C* **33**, 560 (1986)
[41] R Vandenbosch and J R Huizenga, *Nuclear fission* (Academic, New York, 1973)
[42] A Bohr, *Proceedings of the United Nations International Conference on the Peaceful Uses of Atomic Energy* (United Nations, New York, 1956), Vol. 2, p. 151
[43] I Halpern and V M Strutinsky, *Proceedings of the United Nations International Conference on the peaceful Uses of Atomic Energy* (United Nations, Geneva, 1958), Vol. 15, p. 408
[44] M G Itkis *et al*, *Phys. Part. Nuclei* **19**, 701 (1988)
[45] F Videback *et al*, *Phys. Rev. C* **15**, 954 (1997)
[46] M Ogihara *et al*, *Z. Phys. A* **335**, 203 (1990)
[47] D P Singh *et al*, *Phys. Rev. C* **80**, 014601 (2009)
[48] B R Behera *et al*, *Pramana – J. Phys.* **57**,199 (2001)